The Effects of Neutron and Gamma Radiation Fields on the Electrical Breakdown Properties of Liquid and Gaseous Helium in Fusion Reactor Superconducting Magnet Systems

L.J. Perkins

September 1983

UWFDM-435

FUSION TECHNOLOGY INSTITUTE

UNIVERSITY OF WISCONSIN

MADISON WISCONSIN

The Effects of Neutron and Gamma Radiation Fields on the Electrical Breakdown Properties of Liquid and Gaseous Helium in Fusion Reactor Superconducting Magnet Systems

L.J. Perkins

Fusion Technology Institute
University of Wisconsin
1500 Engineering Drive
Madison, WI 53706

http://fti.neep.wisc.edu

September 1983

UWFDM-435

THE EFFECTS OF NEUTRON AND GAMMA RADIATION FIELDS ON THE ELECTRICAL BREAKDOWN PROPERTIES OF LIQUID AND GASEOUS HELIUM IN FUSION REACTOR SUPERCONDUCTING MAGNET SYSTEMS

L. John Perkins

Fusion Engineering Program
Nuclear Engineering Department
University of Wisconsin-Madison
Madison, Wisconsin 53706

September 1983

UWFDM-435

CONTENTS

ABSTRACT

In the event of a serious disruption in a superconducting magnet, a rapid discharge of the stored energy is necessary leading to appreciable induced voltages in the system. The rate of discharge must be limited to below that which would cause electrical breakdown of the helium coolant (the weakest dielectric in the system) otherwise partial or total coil destruction may occur. However, in a fusion reactor environment, the superconducting magnets are exposed to appreciable neutron and gamma fluxes. It is demonstrated in this study that such radiation fields are potentially capable of significantly reducing the currently established (i.e., unirradiated) electrical breakdown potentials of helium and, accordingly, a formal theory of this radiation-induced breakdown phenomenon has been developed to explicitly describe the reduced breakdown potentials in terms of the incident radiation spectrum.

In this report it is shown that the conventional Townsend theory of electrical breakdown is not equipped to deal with radiation-induced ionization and the current theory is extended to include external radiation fields. In particular it is shown that radiation effects will be significant if the dose-rate-induced equilibrium ionization density in the helium medium is comparable to the critical ionization density required for spark-streamer formation. Application of the analysis to the superconducting magnets of the WITAMIR-I tandem mirror reactor provides a time-dependent description of the radiation-induced ionization densities in the gaseous and liquid helium substrates and, thereby, relates the reduced breakdown potentials to the incident radiation field.

Particular emphasis is given to the implication of these results including the future deployment choices of superconducting magnet cryogenic methods (e.g., pool-boiling versus forced-flow, etc.), the possible impact on shielding requirements for superconducting magnets, and the analogous situation for radiation-induced electrical breakdown of insulating gases in pressurized waveguides and coaxial feeds for fusion RF heating systems.

1. INTRODUCTION AND SYNOPSIS

Large superconducting magnet systems constitute a major component in current engineering designs of conceptual magnetically-confined fusion reactors.[1-3,49] Such magnet systems are characterized by large current densities (kiloamperes cm^{-2}) and large inductances (several henrys) and, therefore, by large associated values of stored energy (gigajoules). In the event of a serious magnet disruption, e.g., the increasing propagation of a normal zone leading to quenching, rapid discharge of the magnet is necessary to prevent a deleterious temperature rise in the system. However, in such a discharge, the rapid reduction of the supply current leads to the induction of large back EMFs in the system. In addition, under normal operation, the occurrence of turn to turn shorts between the normal-conducting stabilizer of the magnet can yield similar large induced voltages. Such voltage surges are directly capable of producing electrical breakdown of the local insulation in the magnet and may lead to partial or total coil destruction.

In this connection, it is important to note that the helium coolant is usually the weakest dielectric in the superconducting magnet assembly. Therefore, an accurate knowledge of the electrical breakdown properties of this medium is a vital factor in the successful design of superconducting magnet systems.

However, the magnet systems in a fusion reactor are exposed to appreciable radiation fields mainly in the form of neutron and gamma radiation. Current experimental evidence which will be reviewed later in this report suggests that external radiation fields are capable of significantly reducing the electric breakdown strength of some gases. Any explanations which were

offered in these studies were qualitative in nature and do not permit the prediction of equivalent radiation-induced breakdown criteria in comparable systems. For the case of helium (both gas and liquid) there is no practical data on this important effect. In addition, to this author's knowledge, no quantitative analysis of the effect of external ionizing agents on the electrical breakdown properties of a dielectric has ever been performed.

In this context of radiation-induced electrical breakdown in fusion reactor systems, one other important factor should be noted. The last five years or so has seen rapidly growing interest in the fusion community in the utilization of radiofrequency (RF) waves. The major use of RF energy for plasma heating has been expanded by its capacity for sustaining current drive in tokamaks and for potential enhancement and thermal barrier maintenance in tandem mirrors. However, with the exception of the novel quasi-optical launcher[4] for electron-cyclotron resonance heating (ECRH) systems, all other conceptual RF power transmission systems rely on waveguides or coaxial feeds containing pressurized insulation gas (usually N_2 or SF_6) to prevent voltage breakdown. As these transmission systems approach the wave launching point at or near the reactor first wall, the neutron and gamma radiation fields within the pressurized guide will be at least as intense as those at the superconducting magnets and, in most cases, considerably more so. Therefore, similar considerations of radiation-induced electrical breakdown will be expected to apply.

It is the purpose of this report, therefore, to examine the influence of external radiation fields on the electrical breakdown strengths of dielectric media, with special emphasis being given to gaseous and liquid helium.

In Chapter 2, the rather scant attention given to this subject in the literature is reviewed and the evidence for radiation-induced breakdown of some gases is collated.

An overview of the currently accepted mechanisms for electrical breakdown is presented in Chapter 3 and the lack of an adequate understanding of these physical processes is underlined.

In Chapter 4, a brief review of electrical breakdown in gaseous and liquid helium in the absence of radiation fields is presented. Particular attention is focussed on those physical properties of the liquid and gaseous media which will determine the efficiency of radiation-induced breakdown.

In Chapter 5, the current theory of electrical breakdown is extended, for the first time, to incorporate the effects of external radiation fields. The chapter begins with a critique of the current postulates of the mechanisms for breakdown and it is shown that the conventional Townsend theory is not equipped to deal with the phenomenon of radiation-induced ionization. A new hypothesis is then proposed in terms of the critical ionization density N_c required for the Townsend avalanche mechanisms to progress to the space-charge limited streamer mechanisms at breakdown. In particular, it is shown that radiation effects will be significant if the radiation-induced equilibrium ionization density N_o is comparable to this critical ionization density N_c required for streamer formation. Expressions are then introduced which relate the reduced breakdown potential to the radiation-induced equilibrium ionization density N_o.

In Chapter 6, the interaction of neutron-gamma radiation fields with the helium subsystem of fusion reactor superconducting magnet assemblies is described. In the general analysis which follows, a differential equation is

constructed and solved to describe the temporal behavior of the neutron-induced ionization densities in both the gaseous and liquid helium coolant, therefore permitting the reduced breakdown potential to be obtained explicitly in terms of the incident neutron spectrum. Application of the analysis to the central cell coils of the WITAMIR-I tandem mirror reactor (a typical fusion reactor superconducting magnet system) demonstrates that the equilibrium value of the neutron-induced ionization density is precisely in the range required to exert a significant influence on the breakdown potential of the helium medium. This application is shown to have additional relevance to other fusion magnet systems. It is stressed that although the fusion plasma would be shut off before a magnet discharge is attempted, the electron-ion recombination coefficient for helium has a uniquely low value with the result that, depending on the helium conditions, radiation-induced ionization densities can remain present for up to tens of seconds after the plasma (and, therefore, the radiation source) has been extinguished. Particular emphasis is given to the implications of these results including (a) the deployment choice of magnet cryogenic systems (pool-boiling versus forced-flow supercritical), (b) radiation-induced breakdown in the toroidal field coils of the less conservative tokamak representative designs, and (c) the analogous situation for radiation-induced breakdown of insulating gases in pressurized waveguides and coaxial feeds for RF plasma heating systems.

Finally, in Chapter 7, the paucity of adequate breakdown-related parametric data for helium, particularly liquid helium, in a radiation environment is underlined and the urgent need for their experimental determination is stressed.

2. A REVIEW OF THE CURRENT EVIDENCE FOR RADIATION-INDUCED BREAKDOWN OF GASES AND LIQUIDS

The influence of external ionizing agents on the breakdown behavior of gases and liquids has received little attention in the literature. The few studies which have been performed in this area are outlined below and prove to be rather inconclusive with regard to the significance of the effect. However, in the majority of these cases, the radiation sources employed were either of low intensity or yielded particles with low specific ionization (i.e., low ionization energy deposited per unit path in the medium).

Allibone and Dring[5] used a 100 mCi gamma ray source which produced several hundred ion pairs cm^{-3} s^{-1} to determine the effect of irradiation on the breakdown voltage in air. (Natural ion production rate, by cosmic ray interactions, etc., would be ~ 1-10 cm^{-3} s^{-1}.) They obtained a reduction in breakdown potential of ~ 10% for some electrode configurations over that for no irradiation. They were also able to show that the standard deviation in the spread of breakdown potentials about the mean value could be reduced, by irradiation, from 10% to 3%. In conclusion, Allibone and Dring recommended that air spark gaps be irradiated with a gamma ray source of approximately 10 mCi for precise specification of sparkover voltage V_s. A weaker source would be insufficient to reduce scatter in V_s while a stronger source would be likely to reduce V_s significantly.

Boylet and Williams[6] have suggested that external irradiation will produce a secondary mechanism in addition to those of the internal secondary Townsend processes during the growth of a discharge. The Townsend process of discharge will be considered later.

Fuchs and Schumacher[7] using external UV irradiation found, for several gases, a reduction in breakdown voltage proportional to the square root of the initial ionization current. For air, Blair et al.[8] found a reduction in breakdown voltage with radium irradiation (an alpha and gamma emitter), but not in proportion to the square root of the measured initial ionization current.

Fallou et al.[9] performed experiments on the breakdown voltage of both liquid and gaseous helium at atmospheric pressure. This study indicated that irradiation had a large effect. The introduction of ^{192}Ir (a beta emitter) onto one electrode lowered the breakdown potential for gaseous helium in the temperature range 5-20 K by as much as 35%! The source strength of the ^{192}Ir source was not stated, neither did the authors attempt a physical explanation of this significant effect.

In a study of laser irradiation of a spark gap in air, Guenther and Bettis[10] showed that the breakdown potential for the gap could be reduced by at least 50%. They also demonstrated that the time delay between the application of the laser pulse and the occurrence of breakdown increased from $\sim$ 5 ns in the case of the application of 95% of the full breakdown potential, to $\sim$ 400 ns for the application of 50% of the full breakdown potential. Similar results were obtained by Morgan and Grey-Morgan,[11] where laser irradiation of an air spark gap reduced the breakdown voltage by approximately 30%.

The phenomenon of electrical breakdown induced by ionizing radiation in gases has been applied in the field of high energy nuclear physics in a class of particle detectors called spark chambers. Here, a uniform field is applied across a gas (usually an inert gas, e.g., He or Ne) by a stacked array of parallel plate electrodes (see for example Ref. 12). The passage of a high

energy charged particle through the detector causes the gas to break down preferentially along the ionization path of the particle. A photograph of the resulting spark enables a record of the path of the particle to be obtained.

The specific ionization deposited by the incident particle in a spark chamber (i.e., the ionization energy deposited per unit path, dE/dx) is of considerable importance regarding the efficiency of spark formation. The more primary ionization electrons produced per unit distance along the path of the particle, the faster will be the creation of the initial avalanche and the brighter the resulting spark will be (see for example Ref. 13). Galaktionov et al.[14] have shown that for a two fold increase in the specific ionization of the incident particle, the luminosity of the resulting spark track is increased between two and three orders of magnitude.

It should be noted here that the specific ionization induced by a high energy particle in a typical spark chamber is much lower than that induced by the alpha particles which result from fusion neutron irradiation of helium gas or liquid. This factor will be discussed in detail later, although it can be seen here that a significant intensity of the latter might be expected to have an appreciable effect on the breakdown properties of helium.

Probably the best demonstration of the dependence of the electrical breakdown of a gas on the specific ionization of the incident radiation is provided by the spark counter, an early predecessor of the spark chamber discussed above. Here, a thin wire anode is suspended in air approximately 1 mm above a metallic plate cathode. A potential of ~ 3 kV is maintained between anode and cathode. (Examples of spark counters can be found in Refs. 15 through 17.) The passage of a heavy charged particle (e.g., a proton or alpha particle) through the high field region surrounding the anode causes breakdown

of the gas with the resulting passage of a spark between anode and cathode. The spark counters constructed by both Connor[16] and Chang and Rosenblum[15] were very sensitive to alpha particles even for very low intensities. However, the counters were almost completely insensitive to gamma or beta emitting sources even for very high intensities, demonstrating that the sparking probability was strongly dependent on the specific ionization of the incident particle in the sensitive region of the detector.

It is important to note here that no studies have every been reported on the effect of external neutron irradiation on the electrical breakdown properties of gases or liquids.

3. A DISCUSSION OF THE CURRENT THEORIES OF ELECTRICAL BREAKDOWN

3.1 Introduction

It is useful here to briefly discuss the currently accepted physical interpretation of electrical breakdown. This theory will be extended in Chapters 5 and 6 to suggest mechanisms by which external radiation can reduce the accepted values of the breakdown potential and where special emphasis will be given to helium.

It should be noted here that even for the simple case of electrical breakdown in uniform fields at moderate gas densities, the general physical mechanism is not well understood. Consequently, varied (and sometimes disparate) physical interpretations of experimental breakdown phenomena may be found in the literature.

3.2 The Townsend Avalanche

The physical cause of breakdown in a liquid or gas lies in the electrical conditions which permit a small electron current to increase to large values whose magnitude is practically limited only by the external circuit. For breakdown to occur, two conditions must be satisfied:

- There must be one or more initiatory electron-ion pairs suitably placed in the medium. These might be produced, for example, by cosmic ray interactions or field emission from the cathode, etc. In the absence of an initiatory electron, a discharge will not develop immediately even though the applied electric field greatly exceeds the breakdown field. In this circumstance, it is necessary to await the arrival of an electron liberated by some means.

- The applied field must be of a sufficient strength and duration to ensure that the initiatory electron(s) generate a series of avalanches such that the amplification by multiplication of electrons and ions offsets the loss by diffusion, recombination or drift out of the electrode space.

It should be noted here that there is a fundamental difference in the mechanism for breakdown in low pressure gases (pressure $\lesssim$ 0.2 atm) and higher pressure gases (pressure $\gtrsim$ 0.2 atm) or liquids. The former occurs preferentially by the Townsend avalanche process, where collisional ionization of the gas molecules by electrons accelerated under the applied field yield an avalanche-type increase in the overall electron density. Secondary contributions to the avalanche occur as the result of positive ion and photon interactions at the cathode. In the latter regime (pressure $\gtrsim$ 0.2 atm), the initial portion of the discharge also proceeds by Townsend electron multiplication. However, because of the large molecular number densities in liquids or gases at higher pressures, space charge limiting of the electron avalanche occurs. At this stage, recombinant photo-ionization processes within the bulk of the gas or liquid dominate and the discharge progresses by the formation of a conducting sheath of luminous plasma known as a streamer.

The significant parameter for the behavior of electron avalanches in a dielectric is E/n, where E is the applied electric field and n is the number density of the medium. This parameter defines the mean energy and the energy distribution of an electron swarm. If E/n is varied in a breakdown experiment, the measurements will relate to a different avalanche condition.

Following Townsend,[18,19] the optimum method for obtaining information on the breakdown mechanism is to measure the ionization current I below breakdown as a function of the gap width d for a constant valve of E/n. Thus, as d is

increased, the applied potential V is increased to keep E = V/d and thus E/n constant. As d is increased, at constant E/n, the increase of current with d is initially exponential, but at larger separations becomes greater than exponential until sparking occurs at some well defined distance d_s. This is shown schematically in Fig. 1 for different values of E/n.

Townsend[18,19] employed a UV source illuminating the cathode to produce the initial low intensity ionization current I_0 in the gas. From an empirical fit to the curves relating I to d, he deduced the relationship

$$I = \frac{I_0 e^{\alpha d}}{1 - (\omega/\alpha)(e^{\alpha d} - 1)} \tag{1}$$

where I_0 = initial ionization current due to external source

d = gap width

α = first Townsend coefficient

ω/α = second Townsend coefficient.

From Eq. (1), there is a value of d (say d_s) which makes the denominator zero such that as $d \to d_s$, then $I \to \infty$. This is the unstable condition at which sparking occurs, thus the spark distance d_s is defined by the breakdown criterion:

$$1 - (\omega/\alpha)\,(e^{\alpha d_s} - 1) = 0\ . \tag{2}$$

The first and second Townsend coefficients (α and ω/α) represent the probability of avalanche production by the primary process (electron ionization) and the secondary processes (positive ion ionization, excitation-photon ionization, etc.), respectively, and are considered further in Section

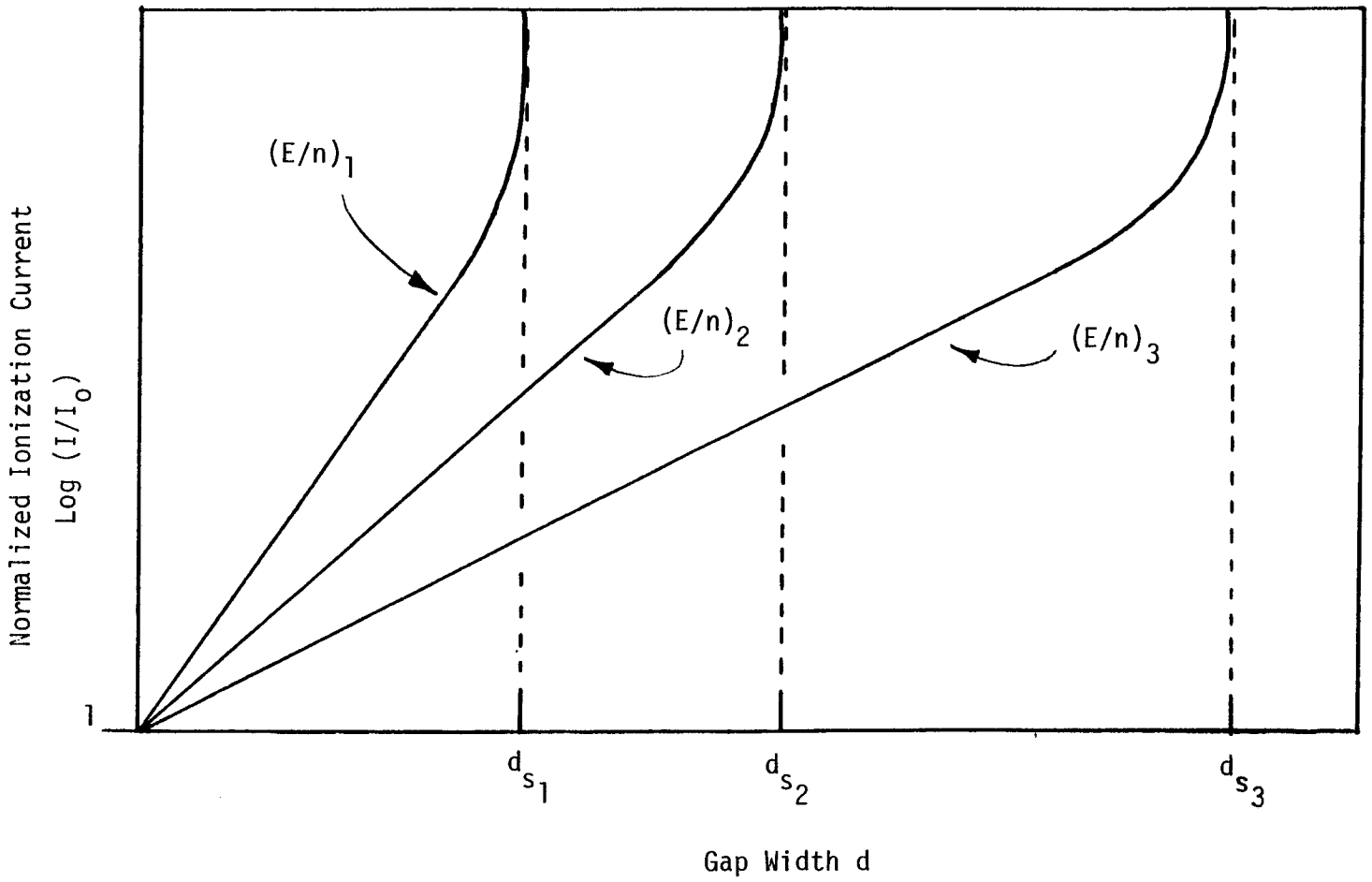

Figure 1 The Growth of the Pre-Breakdown Ionization Current at the Approach to Breakdown, for Constant Values of E/n.
$[(E/n)_1 > (E/n)_2 > (E/n)_3]$

5.2. Both of these parameters are specific functions of E/n, i.e. $\alpha = f(E/n)$ and $\omega/\alpha = g(E/n)$, thus Eq. (2) enables the breakdown potential V_s (= Ed_s) at d_s to be determined.

Paschen's law[20] follows directly from Eq. (2). Placing $\alpha = f(E/n)$ and $\omega/\alpha = g(E/n)$ in Eq. (2), together with $V_s = Ed_s$ yields the result that the breakdown potential V_s is a function only of the gap d_s at breakdown and the number density n of the medium, i.e.,

$$V_s = F(nd_s) \ . \tag{3}$$

The physical interpretation of Eqs. (1) through (3) is that for a constant E/n, increasing d provides an increase in the total amount of ionization produced with distance. At a critical value, d_s, the ionization has multiplied sufficiently to cause breakdown. Thus for any value of E/n, no matter how small, there exists a value of d_s, however large, at which sufficient multiplication has occurred to cause breakdown. It should, therefore, be noted that the value of the electric field E at which breakdown occurs is not a constant for a given gas or liquid containing a given number density of constituent molecules/atoms, since it will vary with the gap width d. Generally, the value of E at which breakdown occurs decreases with increasing d (see for example Refs. 21, 22 and 23).

3.3 Extension to Streamer Formation

As mentioned above, it was necessary to extend the theory of the Townsend electron avalanche process in gases of pressures greater than ~ 0.2 atm, or in liquids, to incorporate the streamer mechanism. This was due to the fact that the narrow luminous sparks observed at breakdown in such media evolved with

formation velocities of $\sim 10^8$ cm s^{-1} whereas measurement of electron mobilities indicated that complete breakdown due solely to the Townsend electron avalanche would take approximately one to two orders of magnitude larger (see for example Refs. 24 and 25).

Several theories of streamer formation have been given in the literature (see for example Refs. 26, 27 and 28). All are qualitative in nature and a systematic quantitative theory has yet to be given. Following Ref. 28, a brief discussion of the streamer model follows below and should be read in conjunction with Fig. 2.

In the electric field, initiatory electrons gain sufficient energy to cause secondary ionization by means of the Townsend multiplication process. The electrons travel rapidly towards the anode away from the lethargic residual positive ions moving relatively slowly in the opposite direction. As this Townsend discharge progresses, the space charge field E_{sc} of the separating electrons and ions becomes important (Fig. 2a). When the number of electrons in the head of the avalanche approaches $\sim 10^6$, the avalanche begins to slow due to the attraction of the positive ions. At $\sim 10^8$ electrons in the head, the avalanche is much restrained,[25] and the space charge field E_{sc} in the middle of the avalanche practically negates the applied field E. As a consequence, electron-ion recombination occurs within the avalanche and resulting UV photons are emitted isotropically. These photons are thus capable of creating ionization in the region surrounding the primary avalanche (Fig. 2b). Those seed ion pairs so produced at the head and tail of the avalanche experience a region of enhanced electric field, while those to the side experience a reduced field. As a result, the electrons freed at the head and tail of the avalanche will accelerate quickly to produce new avalanches (Fig. 2c), for the

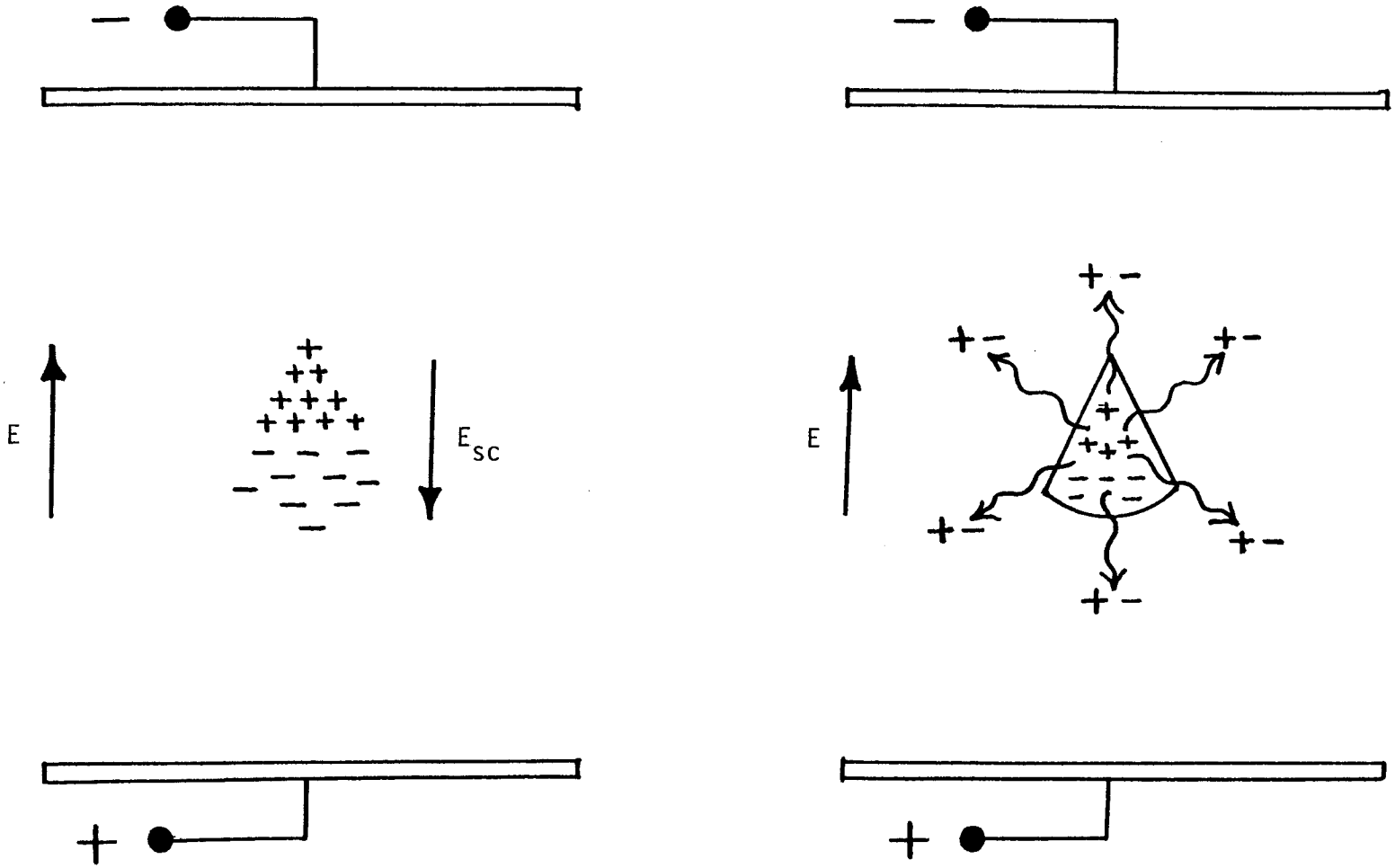

2a. Motion of electrons generated by the Townsend avalanche is space charge limited by the internal field E_{sc}.

2b. UV photons are emitted from internal electron-ion recombinations and create seed ion pairs surrounding the initial avalanche.

Figure 2 The Streamer Mechanism
(figure continued over)

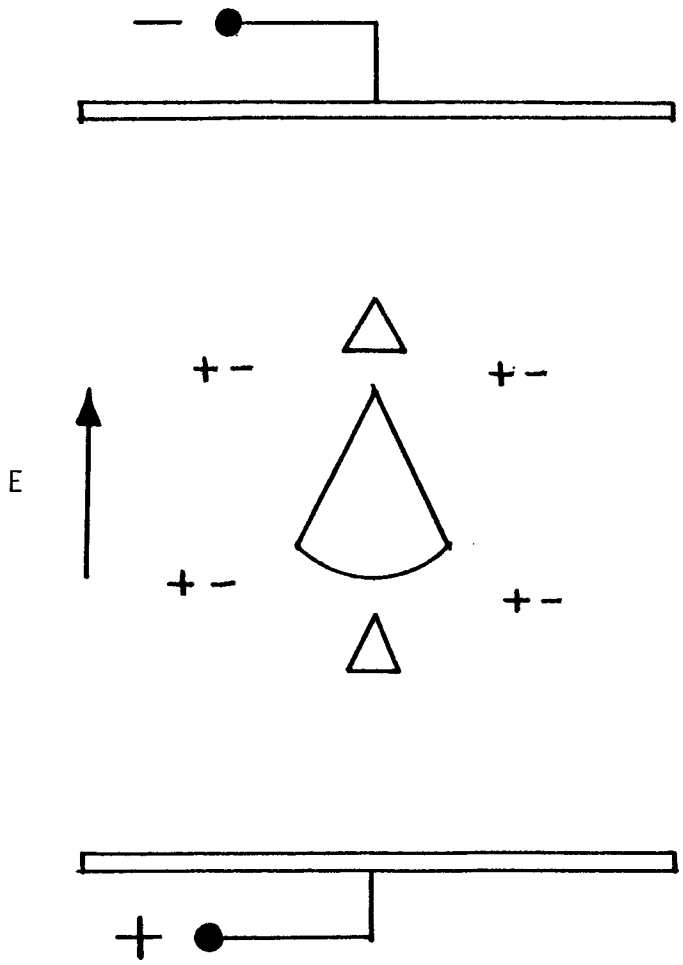

2c. New avalanches rapidly propagate at the head and tail of the original avalanche due to the enhanced local field regions there.

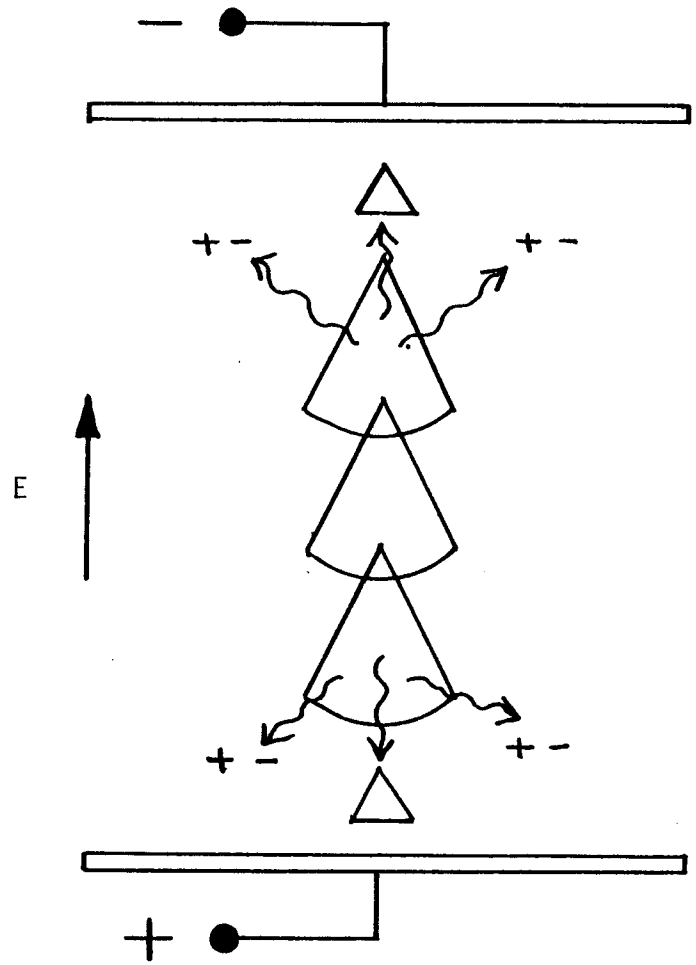

2d. New avalanches also become space charge limited and merge with old avalanches to form a streamer propagating predominantly by photon transport.

first Townsend coefficient α depends on the local value of the electric field, $\alpha = f(E/n)$. These new avalanches grow until they are large enough to repeat the process. The old and new avalanches merge into each other to form a streamer whose extremities advance towards the anode and cathode at a speed of $\sim 10^8$ cm s^{-1} (Fig. 2d). On arrival, the electrodes are connected by a low resistance plasma of electrons and ions and along which a spark current can pass.

It should be noted that the conducting path of the streamer has been burned by photon transport linking individual electron avalanche regions. No single electron has crossed the gap.

4. AN OVERVIEW OF ELECTRICAL BREAKDOWN IN GASEOUS AND LIQUID HELIUM IN THE ABSENCE OF RADIATION FIELDS

4.1 Introduction

Thus far, the discussion of the phenomenon of breakdown has not been limited solely to helium. Before the theory is extended to include the effect of radiation fields, it is instructive here to review some of the properties of liquid and gaseous helium which may determine the efficiency of radiation-induced breakdown.

4.2 Breakdown in Gaseous Helium

Gaseous helium at ambient temperatures and pressures is by far the weakest dielectric in a superconducting magnet system. For example, the breakdown potential for a 1 cm gap in helium gas at 1 atm and 300 K is only ~ 2.07 kV.[23] This should be compared with ~ 30 kV for dry air at the same temperature and pressure.

The reason for this low dielectric strength is that helium, being a monatomic gas, has no low energy excited molecular states. It is therefore probable that incident electrons will gain energy by elastic collisions with helium atoms. Thus, the relatively high ionization energy of 24.48 eV is likely to be built up over the course of several collisions. By contrast, in polyatomic gases (e.g., O_2), electrons are likely to lose energy on collision with the gas molecules, such that inelastic collisions without ionization (i.e., excitation only) is more likely.

A second contributor to the low breakdown potential is the inability of helium (as in all inert gases) to form negative ions (He^-) by electron attachment.[29] However, the addition of very small amounts of an electronegative

impurity (e.g., O_2) to helium at ambient temperatures can yield a very large increase in the breakdown strength. The effect of such impurities on the breakdown strength of helium liquid or gas at low temperatures is negligible since they freeze out.[22]

Although the breakdown potential in gaseous helium is small at ambient temperatures, it rises with decreasing temperature at constant pressure (i.e., with increasing density), reaching a value of ~ 75 kV for a 1 cm gap at T = 4.2 K.[23] In the liquid state, the electron drift velocity is at least two orders of magnitude less than that for helium gas, which results in a significant further increase in the breakdown strength.

4.3 Breakdown in Liquid Helium

There have been several studies published on the breakdown potential of liquid helium. Whereas the equivalent studies on gaseous helium are in reasonable agreement, the reports on liquid helium exhibit diverging and rather conflicting results (see for example Refs. 5, 9, 21-23, 30-33). In addition, the individual measurements for V_s in the liquid state show rather poor reproducibility, a large scatter being associated with the data points (see for example Ref. 9).

Paschen's law ceases to hold in gas densities greater than ~ 0.016 g cm^{-3} [9,21,22] (equivalent to a temperature of ~ 4.5 K at 1 atm). Above this density, the breakdown shows a rapid rise with decreasing temperature and another rapid rise as the liquid phase is formed.

The variation in the quoted values of the breakdown strengths in liquid helium is probably due to the different states of the liquid employed. Meats[22] has shown that the breakdown potential rises with increasing pressure over the liquid, while Gerhold[21] states that liquid breakdown is independent

of pressure and temperature, provided the liquid is held near saturation so that bubble formation is inhibited. Therefore, where pool boiling helium is employed, rising gas bubbles are likely to initiate breakdown due to their relatively low density; in this case only the breakdown strength of the saturated vapor should be relied on. In the case of forced flow cooling, the breakdown strength of liquid helium in the supercritical state can be employed (e.g., ~ 400 kV cm^{-1} for a 0.5 cm gap[23]).

Where vapor bubble formation is inhibited, Meats[22] has suggested that fundamentally different mechanisms may be occurring in the liquid to account for the drastic reduction in electron mobility. Here it is proposed that interactions between free electrons and helium atoms in the liquid create "pseudo bubbles" of radius ~ 5 x 10^{-7} cm which form localized electron cavities. Breakdown then proceeds by way of the Krasucki effect.[34]

Williams[30] has suggested that helium in the liquid state is capable of supporting negative ion formation. This suggestion followed from the fact that the existence of molecular states of helium at the high liquid densities had been proposed. Such states may therefore be capable of attaching free electrons, and would account for the high breakdown potential exhibited by liquid helium.

4.4 Free Electron Behavior in Helium

Electron multiplication in the liquid phase of the inert gases has also received attention due to their incorporation as the sensitive volume of liquid radiation detectors (see for example Refs. 35, 36). The significant fact here is that the liquid (and solid) phases of the inert gases are the only known condensed dielectrics, other than semiconductors, in which electrons remain free. Therefore, the high density of the liquid gas is a

great advantage in respect of the efficiency with which the incident radiation can be detected. This phenomenon of a very low recombination rate of electrons, once formed in pure helium, is of great importance since large charge densities may be built up by external ionizing radiation; this aspect will be fully discussed in Chapter 6.

In helium gas, electrons may remain free for tens of microseconds or more.[37] In helium liquid, it is likely to be significantly longer. In fact, Dolgoshein[38] discovered that in liquid argon, electrons previously liberated by an ionizing event in the bulk of the liquid showed almost no recombination effects and, when allowed to drift to the surface of the liquid, were emitted into the vapor phase with essentially 100% efficiency!

5. EXTENSION OF THE TOWNSEND THEORY TO PREDICT RADIATION-INDUCED BREAKDOWN

5.1 Introduction

In view of the evidence in Chapter 2, it would appear that current theories of electrical breakdown require extension to account for the breakdown phenomena observed when gases and liquids are exposed to external radiation fields. Any explanations which were offered in those studies referenced in Chapter 2 were qualitative in nature and thus do not permit the prediction of equivalent breakdown criteria in comparable systems. It is the purpose of this chapter to introduce a theory which seeks to quantify the dependence of the breakdown potential of a dielectric on the ionization charge induced by the incident radiation field.

5.2 A Critique of the Townsend Theory of Breakdown

The analysis in Chapter 3 demonstrated that breakdown of a dielectric medium can be said to have occurred when the electrodes are connected by a low resistance conducting plasma. It was shown that the approach to breakdown may be investigated by measuring the electron current I reaching the anode as a function of the electrode spacing d for a constant value of E/n. Performance of this measurement necessitated the creation of an initial low intensity electron current I_0 in the gas by external means (e.g., UV illumination of the cathode, etc.). The current I was seen to initially rise exponentially with slope α for increasing d, the rise becoming more rapid for further increase in d, finally becoming asymptotically infinite at $d = d_s$ and voltage $V = V_s = Ed_s$ (see Eqs. (1) and (2)). For values of d less than d_s, the medium behaves as an insulator and I is proportional to the initial current I_0. When $d = d_s$,

the magnitude of the current is controlled by the series impedance of the power supply.

The primary Townsend process of ionization via electron collision, and parameterized by the first Townsend coefficient α (see Eq. (1)), is not sufficient by itself to cause breakdown. It is, therefore, necessary to also consider the secondary processes, collectively parameterized by the second Townsend coefficient ω/α, which are responsible for further multiplication of the electron current. Depending on the number density of the medium, these secondary processes may occur preferentially in the bulk of the medium (for high pressures $\gtrsim$ 0.2 atm) or at the cathode (for low pressures $\lesssim$ 0.2 atm), and include:

1. Electron secondary emission at the cathode from positive ion bombardment.
2. Electron secondary emission at the cathode due to the incidence of excited atoms.
3. Photoelectric emission at the cathode due to the incidence of excitation photons.
4. Ionization of the medium via positive ions.
5. Ionization of the medium via excitation photons (including the special case of space charge limiting leading to streamer formation -- see Section 3.3).

These secondary processes, whether acting alone or in combination, lead to a growth curve of the form of Eq. (1) and just which of the secondary processes predominates under certain conditions cannot be distinguished simply from the curve. It can be seen, however, that a transition in the dominant secondary processes from cathode-dependent, via medium-dependent, to space charge-dependent (i.e., streamer mechanism) is to be expected as the number

density of the medium is increased. The transition pressure is usually taken as being around 0.2 atm.

Thus, in the absence of a significant external radiation field, a uniform field in helium gas at moderate pressures ($n \lesssim 3.01 \times 10^{21}$ cm^{-3}) possesses a well defined sparking potential V_s which is a function of the gap width d and number density n (see Eqs. (2) and (3)). Here, once some initiating low intensity ionization current I_0 is established, attainment of V_s causes the discharge to self-propagate via the Townsend avalanche followed by the streamer processes until the gap is bridged with a conducting plasma.

However, once the spark is initiated, it is no longer required that the potential be held at V_s for arc conditions to be maintained. In fact, for a 1 cm gap in helium gas at room temperature and 1 atm, the arc is extinguished only when the potential is reduced from the breakdown potential of ~ 2.07 kV down to a value of a few tens of volts.[39] Thus the breakdown potential V_s is only required to provide the initial multiplicative regeneration of the electron current via the Townsend avalanche and streamer mechanisms leading to a conducting plasma column. Once formed, the breakdown channel is self-sustaining until the applied potential is reduced below some relatively low value. It is probable that this low extinguishing potential is the minimum voltage which must be applied to overcome deleterious recombination effects in the body of the plasma.

It is, therefore, important to note that the apparent purpose of the breakdown potential V_s is to produce a sufficient ionization density in the medium so that a breakdown channel is formed and that it is not subsequently required for further ionization once the medium has broken down since the current is then maintained by the external circuit. The vital question, there-

fore, in the case of radiation-induced breakdown, is to what extent does the ionization density induced by an external radiation field reduce the breakdown potential below the full value V_s required in the absence of the incident radiation field?

Modification of the current Townsend theory of breakdown to account for radiation-induced ionization requires recognition of the limitation of the Townsend relationship of Eq. (1):

$$I = \frac{I_0 e^{\alpha d}}{1 - (\omega/\alpha)(e^{\alpha d} - 1)} \quad .$$

This limitation is that, although the equation correctly expresses the multiplication of the ionization current by the primary and secondary processes in the steady state, it does not describe the temporal transition to spark formation. The consequence of this fact is that the criterion for breakdown, defined by Eq. (2) for the value of $d = d_s$ at which $I \to \infty$, i.e.,

$$1 - (\omega/\alpha)(e^{\alpha d_s} - 1) = 0 \ ,$$

is <u>not</u> apparently a function of the initial ionization current I_0 in the medium. Therefore, according to the original Townsend theory, electrical breakdown is <u>not</u> dependent on the initial ionization density in the medium, irrespective of the magnitude of this ionization density, and thus is <u>not</u> influenced by an external radiation field.

The fact that the Townsend theory apparently makes no allowance for the dependence of the breakdown potential on the initial initiation density is due to the fact that the theory was deduced for the special case where the low

value of the initiatory UV ion current I_0 in the medium was many orders of magnitude less than the final ionization density required for breakdown (the latter being produced entirely by the multiplicative processes in the medium).

5.3 Extension of the Townsend Theory

It is possible to resolve this limitation regarding the initial ionization density if the following hypothesis is proposed:

> *That, as the applied potential V or the gap width d is increased, the ionization current I increases to a critical value I_c at which point space charge effects become sufficient for the onset of streamer formation to occur. At the value of I_c, and for no further increase in V, the current multiplies rapidly via the streamer mechanism reaching a value determined by the series impedance in the external circuit. The value of the breakdown potential V_s is thus defined to be that voltage sufficient to cause multiplication by the primary and secondary processes, such that the current attains the critical value of I_c at which point current instability by streamer formation occurs. Therefore, very importantly, if the initial ionization density N_o produced in the medium by the external radiation field is comparable to the critical ionization density N_c required for the onset of streamer production, then the value of the breakdown potential V_s required to produce N_c is reduced accordingly.*

Supportive evidence for this hypothesis is given in Chapter 2. For example, the spark counter maintains its quiescent condition of a stable high potential V on the anode wire when unirradiated or when irradiated by beta or gamma rays of low specific ionization. However, an alpha particle of high

specific ionization entering the sensitive region around the anode wire produces sufficient ion pairs such that the multiplication of these ion pairs by the applied potential V is now large enough to attain the space charge number density N_c required for streamer formation in this system, with the resulting passage of a spark between anode and cathode. This would then explain the requirement in such counters for particles of certain minimum ionization densities necessary for detection by sparking and the fact that they are insensitive to beta and gamma radiation which have low specific ionizing power.

A further example of support for the hypothesis is evident in the case of laser breakdown of spark gaps where it was seen in Chapter 2 that the time delay between the application of the laser pulse and the occurrence of breakdown increased for increasing reduction of the applied potential V below the full breakdown potential V_s. The time delay, therefore, is dependent on the difference between the critical number of charge carriers N_c required for streamer formation and the initial number injected by the laser pulse. Since the streamer mechanism progresses via UV photon transport (see Chapter 3), it is much faster than the Townsend electron avalanche process (up to two orders of magnitude). The time delay for breakdown is then almost solely due to that required for electron multiplication via the Townsend avalanche to reach the critical value N_c for streamer onset and this is dependent on the difference between the full breakdown potential and the applied potential $V_s - V$. The full breakdown potential V_s would only be required as the number of initially injected charges tends to zero (or, at least, tends to a number which is much less than N_c).

5.4 The Modified Breakdown Criterion

It is now necessary to place the modified breakdown criterion on a quantitative footing by predicting the reduction of the breakdown potential from the value V_s given by the conventional Townsend theory to a value $V_s'(N_o)$ which is a function of the initial ionization density N_o induced by the external radiation field.

For those values of the applied potential V or gap width d, for which the ionization current I is less than the critical value I_c required for the onset of streamer formation, the approach to breakdown is correctly expressed by the conventional Townsend relationship of Eq. (1). This relationship may be rewritten in terms of the equivalent ionization densities N and N_o, rather than the ionization currents I and I_o, as follows

$$N = \frac{N_o e^{\alpha d}}{1 - (\omega/\alpha)(e^{\alpha d} - 1)} \tag{4}$$

for constant E/n.

As proposed above, the onset of breakdown occurs at that gap width d_s' at which the ionization current I attains the critical value of I_c (i.e., at which the ionization density N attains the critical ionization density N_c). The modified Townsend breakdown criterion can therefore be expressed as

$$N_c = \frac{N_o e^{\alpha d_s'}}{1 - (\omega/\alpha)(e^{\alpha d_s'} - 1)} . \tag{5}$$

Note that the gap width at breakdown d_s' is written with a prime to distinguish it from the gap width d_s defined by the conventional theory, since it is now defined as a function of the initial ionization density, i.e., $d_s' = d_s'(N_o)$.

In the domain where the initial ionization density N_o is much less than the critical value N_c (i.e., the conventional Townsend domain), Eq. (5) above reduces to the conventional breakdown criterion of Eq. (2) and $d_s' \rightarrow d_s$.

Manipulation of Eq. (5) enables the reduced gap width at breakdown, d_s', to be obtained explicitly in terms of the initial ionization density N_o as follows

$$d_s'(N_o) = \frac{1}{\alpha} \ln \left\{ \frac{1 + (\omega/a)}{(N_o/N_c) + (\omega/\alpha)} \right\} . \tag{6}$$

Therefore, multiplying by the electric field E, the reduced breakdown potential V_s' can be defined explicitly in terms of N_o as follows

$$V_s' (N_o) = Ed_s' = \frac{E}{\alpha} \ln \left\{ \frac{1 + (\omega/\alpha)}{(N_o/N_c) + (\omega/\alpha)} \right\} \tag{7}$$

where d_s' = reduced gap width at breakdown

E = applied field

α = first Townsend coefficient

ω/α = second Townsend coefficient

N_o = initial ionization density from external radiation field

N_c = critical ionization density for streamer formation.

Finally, combining Eqs. (2) and (7) enables the reduced breakdown potential V_s' to be expressed in terms of the full (conventional) breakdown potential V_s as follows

$$V_s' (N_o) = \frac{\ln \left(1 + \frac{\omega}{\alpha}\right) - \ln \left(\frac{N_o}{N_c} + \frac{\omega}{\alpha}\right)}{\ln \left(\frac{\alpha}{\omega} + 1\right)} V_s . \tag{8}$$

The reduced breakdown potential is seen to depend on the ratio of N_o/N_c. If the initial ionization density N_o is sufficiently small such that $N_o << N_c$, then the reduced potential approaches the value of the full breakdown potential V_s predicted by the conventional theory.

If the approach to breakdown is now repeated, where the ionization current I in the medium is measured as a function of the gap width d for a constant value of the multiplication parameter E/n, the schematic curves of Fig. 3 would result for two different values of the radiation-induced initial ionization density, N_{o_1} and N_{o_2} where $N_{o_1} > N_{o_2}$. These yield equivalent initial ionization currents I_{o_1} and I_{o_2}, where $I_{o_1} > I_{o_2}$. Since the parameter E/n is the same for both cases, it is seen that the slopes of the curves are the same for a logarithmic ordinate (current axis). However, since $I_{o_1} > I_{o_2}$, a certain value of d, say d'_{s_1} (and thus a certain value of $V = V'_{s_1} = Ed'_{s_1}$), exists, where the current has increased to I_c and the space charge density is sufficient for streamer formation to occur. The current can now increase to that limited by the external circuit, without further increase in d (or V). Reduction of I_{o_1} to I_{o_2} necessitates a larger value of d, say d'_{s_2} (and thus $V = V'_{s_2} = Ed'_{s_2}$), before the critical current I_c is attained. Reduction of I_o to a small value I_{o_3}, such that $I_{o_3} << I_c$ (i.e., $N_{o_3} << N_c$), necessitates the application of the full breakdown potential V_s predicted by the conventional Townsend theory before breakdown will proceed.

It is important to note here that, because of the large stored energy in fusion superconducting magnet systems, the equivalent "external circuit" can supply very large currents indeed in the event of a breakdown. The resulting arc is then capable of causing severe damage to the magnet.

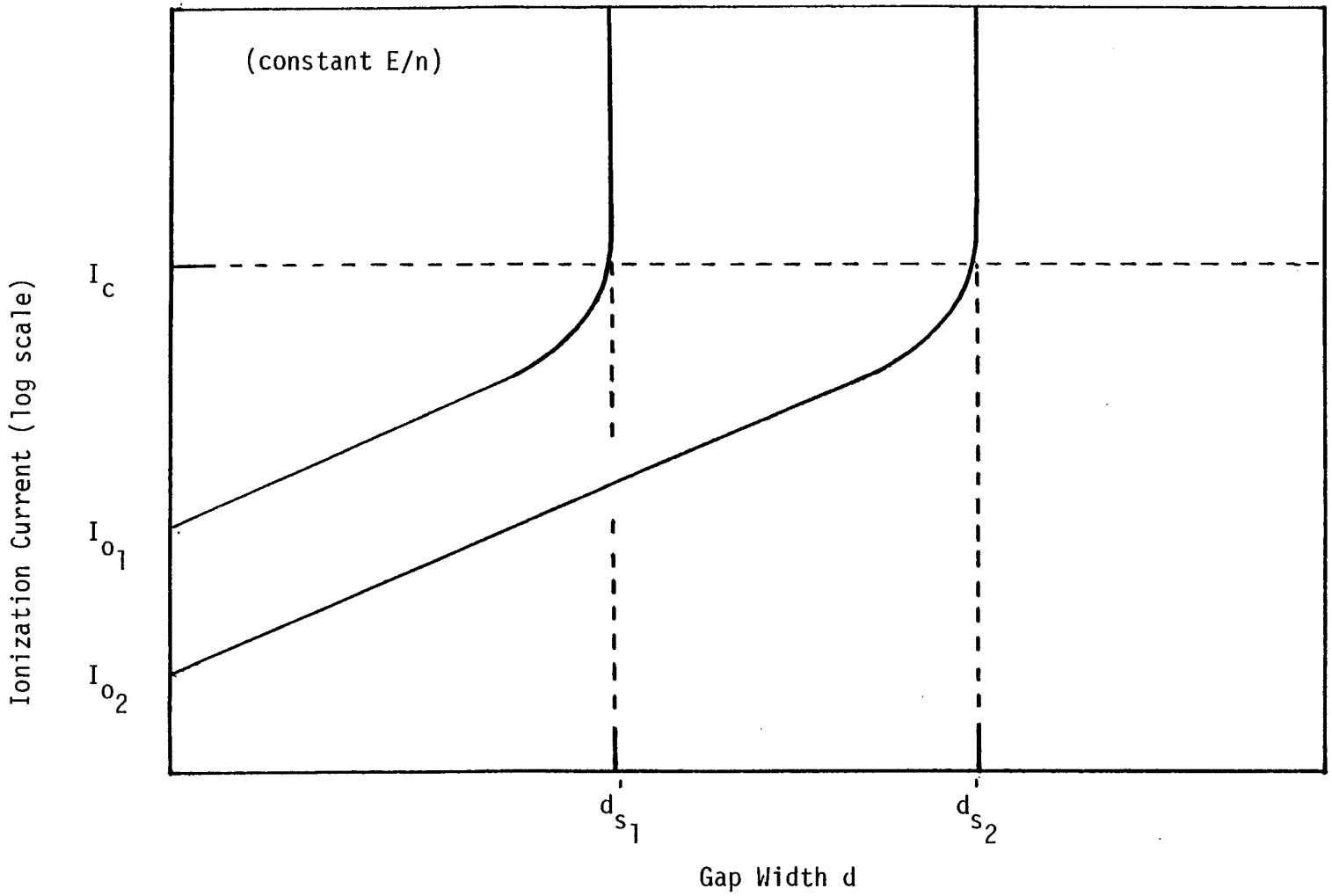

Figure 3. The Approach to Breakdown of the Ionization Currents for the Situation Where the Initial Ionization Densities (N_{o_1},N_{o_2}) are Comparable to the Critical Ionization Density (N_c).

5.5 Quantification of the Critical Ionization Density

It is important here to ask just what is the value of the critical ionization density N_c at which the Townsend discharge becomes space charge limited and the resulting streamer formation leads to breakdown. In Section 3.3, a discussion of the physics of streamer formation indicated that separation of the slowly moving positive ions and the energetic electron avalanche produces an effective internal space-charge dipole field E_{sc} which tends to negate the external field.

Raether[25] has shown that the transition from the avalanche to the streamer occurs when the space charge field is in the range of 0.7-1.0 of the applied field, which corresponds to 10^7-10^8 electrons in the head of the avalanche. Schmitt et al.[40] extended Raether's approach and their calculations indicate that streamer commencement occurs when the space charge field is ~ 0.7-0.8 of the applied field, corresponding to about 10^7 electrons in the avalanche.

Photographs of the initial stages of streamer growth[25,26] indicate that these electrons occupy a volume of ~ 0.1 - 1 cm. This, therefore, infers a critical ionization density of $N_c \sim 10^8$-10^{10} cm^{-3}. Such a value is in agreement with the corresponding parameter for the linear charge density (i.e. line density) generated in a typical streamer, suggested by Wilkinson,[41] of ~ 10^{10} ion pairs per cm.

5.6 Streamer Formation in Highly Non-Uniform Fields

It should be noted that the modified breakdown hypothesis above assumes that breakdown is assured once the streamer mechanism has been initiated and for no further increase in applied potential. From consideration of the streamer mechanism in Section 3.3, this is a good assumption for the case of

breakdown in uniform fields (i.e., cases where the gap width is small compared with the electrode dimensions).

In the case of non-uniform fields (i.e., small electrode dimensions and large gaps), typical photographs of streamer breakdown show characteristic multi-filamentary streamers, some of which are arrested when propagating in a direction away from the central axis of the gap (see for example Refs. 42 and 43). Due to the isotropic emission of UV photons from a streamer, its propagation path can possibly deviate from the gap axis and thus from the direction of the applied field, although multiplication would preferentially occur at the head and tail of the initial streamer due to the enhanced electric fields (see Section 3.3). Thus, in the case of non-uniform fields, production of N_c in the vicinity of the gap axis would appear to be important.

In the case of highly non-uniform fields, it would, therefore, be expected that the value of $V_s'(N_o)$ predicted from the above analysis represents the lower limit of that practically attainable.

6. AN ANALYSIS OF RADIATION-INDUCED BREAKDOWN IN THE HELIUM SUBSYSTEM OF A TYPICAL FUSION REACTOR SUPERCONDUCTING MAGNET ASSEMBLY

6.1 Introduction

In this chapter, an analysis is performed to assess the significance of the radiation field in reducing the electrical breakdown potential in the helium subsystem of a typical fusion reactor superconducting magnet system. In order to classify the effect as significant, it is necessary to show that the steady state ionization density N_0 in the helium cryostat of the magnet, due to the incident radiation field, is comparable to the critical value N_c required for the onset of space charge limiting and thus streamer formation.

6.2 Interaction of Neutron-Gamma Radiation Fields With Helium

Current conceptual fusion reactor designs, operating under the DT fuel cycle, release the majority of their reaction energy to the blanket and shield in the form of 14 MeV neutrons. As they slow down in the blanket/shield assemblies, these neutrons are capable of undergoing elastic, inelastic and non-elastic reactions with the nuclei of the blanket/shield, with the result that the superconducting magnet systems are exposed to a mixed radiation field comprising a continuous neutron and gamma ray spectrum.

The current philosophy in the design of the radiation shields for the superconducting magnets encompasses two criteria (see for example Refs. 44 and 45). First, the flux at the magnets must be less than the critical value which would produce an unacceptable heating rate in the conductors. Maximum power densities are of the order of $\sim$ 0.08 mW cm^{-3} and are determined by economic considerations of cryoplant capacity and shield costs (see for example Ref. 1). Second, the fluence (time integrated flux) must be less than the

critical value which, over the operating life of the reactor, would produce unacceptable radiation damage in the organic insulation (maximum permissible absorbed dose is $\sim 10^{10}$ rads) or produce a deleterious increase in the resistivity in the magnet stabilizer material (annealing is required for a neutron fluence greater than about $\sim 10^{17}$ cm^{-2}).[46]

In the majority of current conceptual fusion reactor designs, cooling of the superconducting magnets is effected by way of helium pool boiling at $\sim$ atmospheric pressure and temperatures in the range 4.2-300 K. The effect of the mixed neutron-gamma field is to cause ionization of this gaseous and liquid helium as described below.

The only interaction which is possible between neutrons of these energies ($\leq$ 14 MeV) and helium nuclei is elastic scattering.[47] Here, the recoil helium nucleus receives a certain fraction of the energy of the incident neutron according to the elastic-scattering differential cross section at this energy, while the total kinetic energy of the interaction is conserved. The resulting recoil helium nuclei, which are by definition alpha particles, have a high specific ionization (i.e., high dE/dx) and lose energy by excitation and ionization of the helium medium. The gamma radiation, by contrast, interacts primarily with the atomic electrons of the medium by way of either the photoelectric, Compton or pair-production effects (see for example Ref. 48). The resulting secondary electrons lose energy to the medium by excitation and ionization of bound electrons in a similar manner to heavy charged particles (e.g., alpha particles). However, because of the small electron mass, the electron paths are tortuous and are characterized by much longer ranges than for heavy charged particles of the same energy. The specific ionization of

the gamma-induced electrons in the helium is, therefore, much less than that for the neutron-induced recoil helium nuclei.

It may be noted that additional radiation sources due to neutron-induced activation of the copper, steel or aluminum matrix of a superconducting magnet assembly are not important here. Maximum saturation activities at the magnets in a typical fusion power reactor are expected to attain values of a few microcuries per watt of operating power (see for example Ref. 49). Such activities of beta-gamma radiation can be neglected when compared with the direct neutron and gamma fields for steady state reactor operation.

6.3 General Analysis

In this section we obtain the differential equation describing the temporal characteristics of the radiation-induced ionization in the helium. The analysis which follows in this section is completely general and may be applied to any system.

It is first necessary to consider how we should treat the separate ionization contributions from the neutron field and the gamma field at the magnets. Consideration of the neutron and gamma spectra at the shielded superconducting magnets of several representative fusion reactor designs,[1-3,49] indicates that the neutron and gamma fluxes at the magnet are approximately comparable in terms of particles cm^{-2} s^{-1}. Consideration of the nuclear heating rate in the bulk material of the magnet typically shows a gamma heating rate which is greater than the neutron heating rate, but within the same order of magnitude. For example, for the central cell magnets in the WITAMIR tandem mirror reactor,[49] the ratio of the gamma heating rate to neutron heating rate in the stabilizer material is ~ 5.6. However, performing a specific comparison of the interaction of the neutron and gamma fields within the gaseous and

liquid helium of the magnet cryostat shows that the ionization density produced by the gamma field in the helium medium can probably be neglected with respect to that produced by the neutron field. This is so for two reasons. First, due to the low atomic number of helium (Z = 2), the probability of all three gamma interaction processes, outlined in Section 6.1 above, is small. (The cross section for the photoelectric and pair-production effects scales as Z^2, while that for the Compton effect scales as Z - see Ref. 48.) Second, the resulting electron produced as a result of a gamma ray interaction has a much lower specific ionization in the helium medium than a recoil helium nuclei (alpha particle) produced by a neutron interaction of the same energy. In fact, the majority of the gamma-induced electrons which initiate ionization in the helium of a typical superconducting magnet will come, not from gamma interactions in the low density helium, but rather from gamma interactions in the surrounding few centimeters of the higher-Z metals which form the bulk of the magnet assembly. The analysis reported here will, therefore, only consider radiation-induced ionization in the helium from the neutron field alone. The calculation will be refined at a later date to include the effect of the gamma field.

The rate of production of ions per unit volume per second due to the slowing down of neutron-induced recoil helium nuclei in the helium medium is

$$S = n \sum_{g=1}^{G} \frac{\sigma_g \phi_g f_g E_g}{W_g} \qquad (9)$$

where n = number density of helium atoms

σ_g = group-averaged microscopic elastic cross section of helium for group g (see below)

ϕ_g = neutron flux in group g (see below)

E_g = midgroup energy for group g

f_g = mean fraction of the neutron kinetic energy in group g imparted to the recoil helium nuclei and dependent on the differential elastic scattering cross section

W_g = mean energy required to create an ion pair in helium by an alpha particle of energy $f_g E_g$

and where the summation is extended over all the G groups comprising the neutron spectrum.

Before proceeding, it is perhaps helpful to define what is meant by "neutron group" in the context of a neutron spectrum. Neutron and gamma spectra at the superconducting magnets of a conceptual fusion reactor are typically computed by multigroup neutron transport methods (see Section 6.4.1 below). Although the neutron spectrum $\phi(E)$ is continuous in neutron energy E, it is necessary in such calculations to discretize the spectrum into a number of discrete energy groups in each of which the neutron energy is constant. Therefore, the multigroup scalar neutron flux in group number g is obtained by the integration of $\phi(E)$ across the group according to

$$\phi_g = \int_{E^{g+1}}^{E^g} \phi(E)\, dE \qquad (10)$$

where E^g and E^{g+1} are, respectively, the upper and lower neutron energy bounds of group g.

The loss of ions in the helium medium will be almost solely due to recombination effects between singly or doubly charged helium ions and free electrons. Very little neutron attenuation takes place across the helium

volume, with the result that recoil helium nuclei are produced uniformly throughout the volume. Loss of ions by diffusion can, therefore, be neglected due to the absence of a concentration gradient. The rate of ion recombination per unit volume can be shown[12] to be proportional to the product of the positive and negative ion number densities N_+, N_-, in the medium according to

$$\left[\frac{\partial}{\partial t} N_+(t)\right]_{loss} = \left[\frac{\partial}{\partial t} N_-(t)\right]_{loss} = - \alpha_r N_+(t) N_-(t) \qquad (11)$$

where α_r is the recombination coefficient. However, in this case, $N_+ \approx N_- = N$ say, thus the balance equation for the electron ionization density in the medium becomes

$$\frac{\partial N}{\partial t}(t) = n \sum_{g=1}^{G} \frac{\sigma_g \phi_g f_g E_g}{W_g} - \alpha_r N(t)^2 \ . \qquad (12)$$

Since the critical ionization density N_c which marks the onset of streamer formation is many orders of magnitude less than the neutral helium number density n, even at ambient temperatures and pressures, it is not necessary to consider the decrease of n in Eq. (12) as positive and negative ions are formed.

The solution of this non-linear differential equation for the time behavior of the ionization density yields

$$N(t) = \left\{\frac{S}{\alpha_r}\right\}^{1/2} \frac{e^{2(S\alpha_r)^{1/2}t} - 1}{e^{2(S\alpha_r)^{1/2}t} + 1} \qquad (13)$$

where, for convenience, we define S as

$$S = n \sum_{g=1}^{G} \frac{\sigma_g \phi_g f_g E_g}{W_g} .$$

When the system has reached steady state, the rate of production of ionization due to the neutron field is equal to the rate of loss due to recombination effects. The equilibrium ionization density in the system then becomes

$$N_o = \left[\frac{n}{\alpha_r} \sum_{g=1}^{n} \frac{\sigma_g \phi_g f_g E_g}{W_g} \right]^{1/2} \tag{14}$$

which forms the initial ionization density parameter required for input to the modified breakdown equations (Eqs. (7) and (8)) in Section 5.4. Substitution of the expression for N_o given by Eq. (14) into Eq. (8), therefore, yields an expression for the reduced breakdown potential V_s' explicitly in terms of the incident neutron spectrum ϕ_g.

One further parameter of interest in this analysis is the time taken by the system to attain a specified fraction of the equilibrium number density N_o. Assuming the radiation field is applied at $t = 0$ and that $N(t) = 0$ for $t < 0$, then the time taken to attain 90% of N_o is

$$t_{90\%} = 1.472 \ (S \ \alpha_r)^{1/2} \tag{15}$$

where S is defined by Eq. (10).

6.4 Application to the Superconducting Magnets of the WITAMIR Tandem Mirror Reactor

6.4.1 Neutronics for the WITAMIR Magnets.

The analysis developed above will now be applied to the superconducting central cell solenoids of the WITAMIR-I tandem mirror fusion reactor. WITAMIR-I,[49] a University of

Wisconsin conceptual design, is a self-consistent DT tandem mirror fusion reactor with thermal barriers. With an operating power of approximately 1500 MW_e, this near term commercial fusion power reactor has a projected time frame of approximately the year 2020 and is envisaged to be the second or third of its kind which will follow the current and planned mirror machines: TMX-U, MFTF-B, FPD and Mirror Demo Reactor.[50] The general reactor parameters of WITAMIR-I are summarized in Table 1.

The central cell of WITAMIR-I has a set of 34 solenoids, 32 of which are identical while two are oversized to provide space for neutral beam heating. The general characteristics of these central cell magnets are summarized in Table 2.

It should be noted that the central cell solenoids of WITAMIR-I are similar in form and function to the toroidal field coils encountered in current designs of near-term and mid-term tokamak fusion devices (e.g., FED,[51] INTOR,[45] UWMAK-III,[1] etc.). In addition, since the neutron wall loading and radiation shielding in both tandem mirror and tokamak reactors are comparable, similar radiation fields would be expected at the magnets. One caveat here, however, is that the WITAMIR central cell magnets were rather "overshielded" in that all radiation limits were more that satisfied. In the case of the MARS tandem mirror reactor,[3] by contrast, the shielding design was optimized such that the radiation limits were just satisfied. Therefore, although analysis of WITAMIR will yield reasonably representative results, it should not be considered a "worst-case" situation.

Coupled neutron-gamma transport calculations were performed on the central cell region of WITAMIR-I employing the one-dimensional discrete ordinates code ANISN[52] with a P_3-S_8 approximation. The central cell, being

Table 1. General Reactor Parameters for the WITAMIR-I Tandem Mirror Fusion Reactor

Thermal Power - MW_{th}	3888
DT Fusion Power - MW_{th}	3000
Plasma Q-Value	28.0
Gross Elec. Power - MW_e	1860
Net Elec. Power - MW_e	1530
Recirculating Fraction - %	18
Net Elec. Eff. - %	39.4
Plug	
Density - cm^{-3}	2.73×10^{13}
Ave. Ion Energy - keV	905
Beta	0.64
Central Cell	
Density, n - cm^{-3}	1.51×10^{14}
Ave. Ion Temp., T_i - keV	32.5
Beta	0.4
Overall Reactor Length - m (w/o DC)	207
Central Cell I.D. - m	1.94
Reactor Structural Material	HT-9
Reactor Coolant	$Li_{17}Pb_{83}$
Breeder Material	$Li_{17}Pb_{83}$
Breeding Ratio	1.07
n Wall Loading, MW/m^2	2.4
Max. End Plug Mag. Field - T	6
S/C - End Plug Material	NbTi
Central Cell Mag. Field - T	3.6
S/C - Central Cell Magnets, Material	NbTi
Barrier Pumping Method	NB
End Plug Beam Energy - keV	500

Table 2. General Characteristics of the Central Cell Superconducting Magnets of WITAMIR-I

Number of coils	32 + 2 oversize for NB access
Major radius	4.3 m
Minor radius	3.3 m
Bundle cross section	1.4 m x 1.0 m
Mean turn length	23.88 m
Volume of winding	33.427 m^3
Weight of winding	88.1 tonnes
Number of turns	1100
Overall current density	950 A cm^{-2}
Ampere turns	13.3 x 10^6 A turns
Self inductance	11.87 H
Self inductance per N^2	9.807 x 10^{-6} H per N^2
Stored energy	0.87 GJ
Field on axis	3.6 T
Max. field at conductor	6.1 T
Superconductor	NbTi
Stabilizing material	Al
Structure material	Al
Helium cryogenic system	Pool boiling at 1 atm
Operating temperature	4.2 K

effectively a long cylinder, lends itself well to 1-D cylindrical modeling. The radial zoning of the blanket-shield-magnet composition of the central cell utilized in the calculation is shown in Fig. 4, where all distances are measured from the central axis of the cylindrical plasma. The transport cross sections employed were a coupled 25-neutron, 21-gamma, group data library condensed from the RSIC DLC-41B VITAMIN-C data library.[53]

The neutron spectrum employed in this analysis is that which is incident on the helium dewar at the inside edge of the central cell magnet - regions K and L in Fig. 4. The spectrum is shown in Fig. 5. Note that this spectrum is in multigroup form as described in Section 6.3 above. The flux units are neutrons cm^{-2} s^{-1} per unit lethargy* and result from a neutron first wall loading in the central cell of 2.4 MW m^{-2}.

6.4.2 Ionization Densities in the Helium Dewar. The analysis performed in Section 6.3 above is completely general and is not specific to the WITAMIR-I magnet system. However, as described in Section 6.4.1, specific results for the WITAMIR-I magnets would be expected to have wide applicability to other fusion magnet systems. Accordingly, the equilibrium ionization density N_0 from Eq. (14), and the $t_{90\%}$ parameter from Eq. (15), will now be evaluated in the helium dewar of the WITAMIR-I central cell magnets. These parameters will be obtained for three different helium conditions of interest to pool boiling cryostats, namely:

- Helium vapor at 1 atm, T = 300 K
- Helium vapor at 1 atm, T = 4.2 K
- Helium liquid at 1 atm, T = 4.2 K

*The lethargy U(E) of a neutron of energy E is defined by $U(E) = \ln (E_0/E)$, where E_0 = 10 MeV.

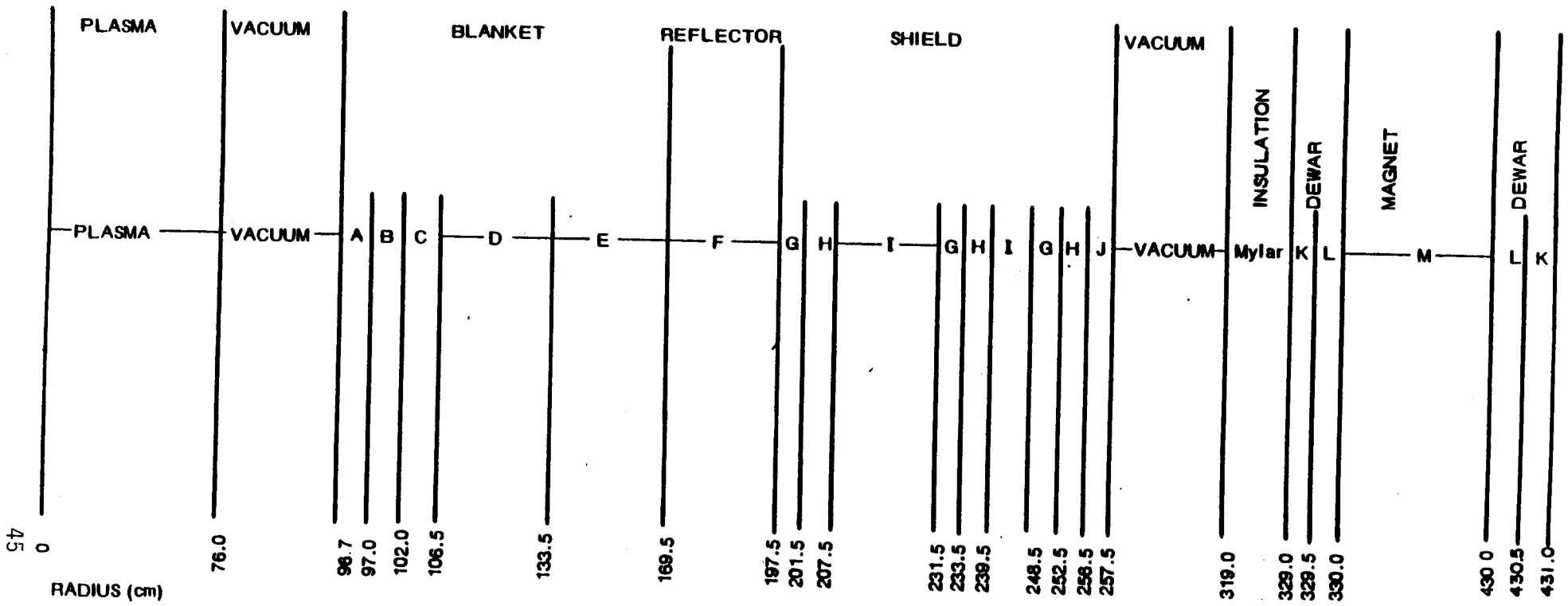

COMPOSITION TABLE

A - 100 % FERRITIC STEEL (HT - 9)

B - 79 % $Li_{17}Pb_{83}$

C - 84 % $Li_{17}Pb_{83}$, 7 % FERRITIC STEEL (F.S.)

D - 81 % $Li_{17}Pb_{83}$, 9 % F.S.

E - 75 % $Li_{17}Pb_{83}$, 25 % F.S.

F - 5 % H_2O, 95 % F.S.

G - 90 % Pb, 5 % H_2O, 5 % F.S.

H - 87 % B_4C

I - 95 % F.S., 5 % H_2O

J - 100 % F.S.

K - 100 % Al 2219

L - 100 % He

M - 17.8 % Al, 69 % Al 2219, 4 % He, 9.2 % INSULATION

Figure 4 The Radial Zoning Employed for the Neutron-Gamma Transport Analysis of the Central Cell of WITAMIR-I

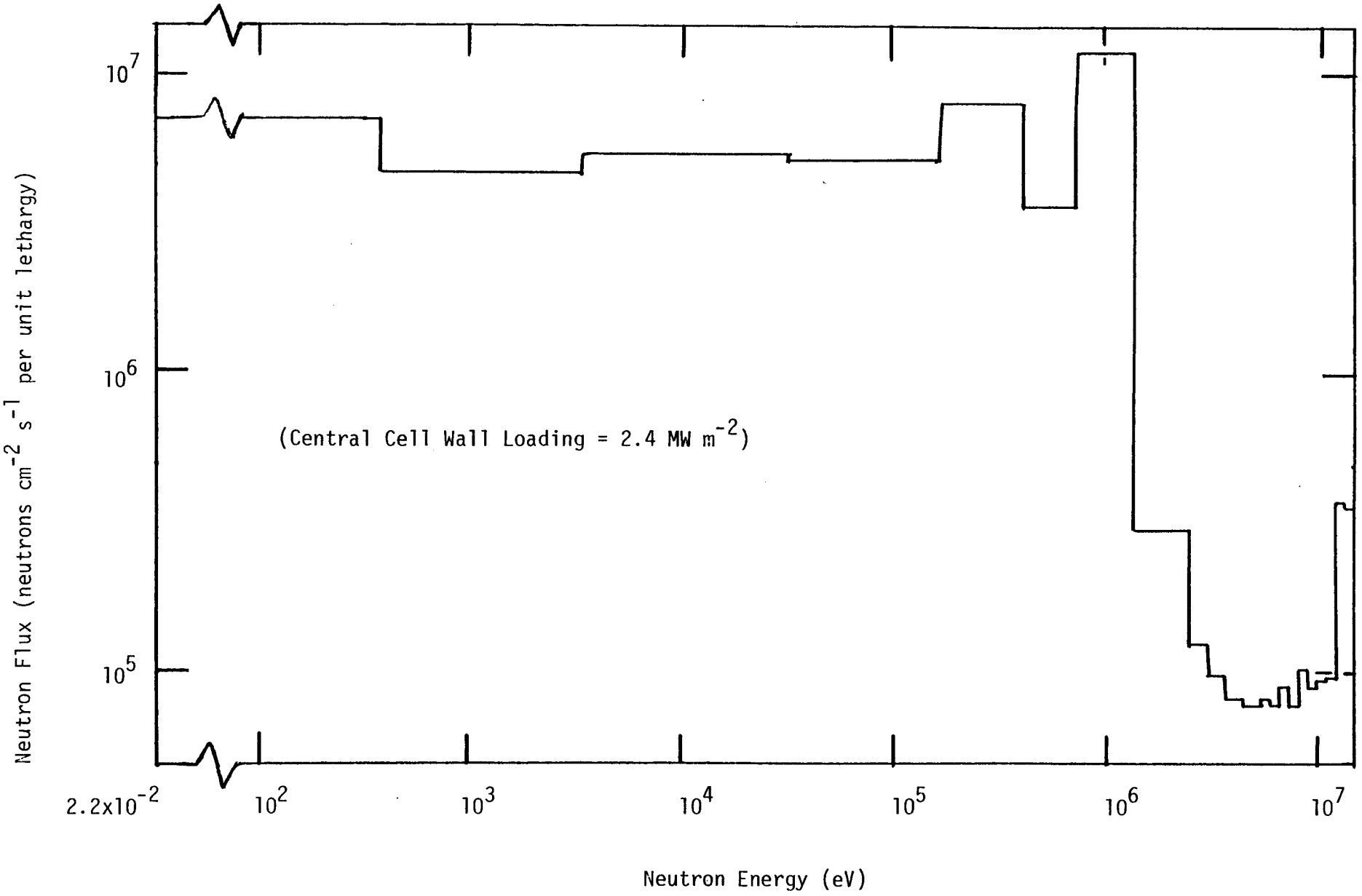

Figure 5 The Neutron Spectrum at the Helium Dewars of the Central Cell Superconducting Magnets of WITAMIR-I

The results are displayed in Table 3 for two different values of the recombination coefficient α_r. As can be seen from Eqs. (14) and (15), both N_0 and $t_{1/2}$ are dependent on $(\alpha_r)^{1/2}$. Unfortunately, precise values of α_r for helium are not available, since systematic experiments to determine this parameter are generally rather difficult to perform. Accordingly, a range of values appears in the literature. For example, Hasted[54] suggests an approximate value of 10^{-8} cm^3 s^{-1}, while Wilkinson[55] suggests a value of 10^{-10} cm^3 s^{-1}. In general, α_r is a function of both the electron number density and the absolute temperature of the medium and values in the above range are indicated.[56] Hence, N_0 and $t_{90\%}$ are evaluated in Table 3 for $\alpha_r = 10^{-8}$ cm^3 s^{-1} and $\alpha_r = 10^{-10}$ cm^3 s^{-1}.

Reference to the results in Table 3 shows that equilibrium ionization densities N_0 in the range 3.6×10^7 cm^{-3} to 2.1×10^{10} cm^{-3} are possible in the helium medium of the WITAMIR-I superconducting magnets under normal reactor irradiation conditions. Corresponding formation time constants (to 90% of N_0) are seen to span the range of 0.069 s to 40 s depending on the specific helium conditions under consideration.

6.5 Discussion of Results and Their Implications

A review of Section 5.5 shows that the critical ionization density N_c required for the onset of streamer formation, and thus breakdown, lies in the range 10^8 to 10^{10} cm^{-3}. Therefore, it would appear that the neutron field of a typical fusion reactor superconducting magnet system is capable of inducing a steady state ionization density N_0 precisely in the range required to exert a significant influence on the breakdown potential of the helium coolant. The initial ionization density N_0, therefore, appears to be directly comparable to the critical value N_c such that, in Eq. (8), the ratio N_0/N_c would produce a

Table 3. Values of the Radiation-Induced Equilibrium Ionization Density for Three Different Helium Conditions

	Helium Vapor at 300 K P = 1 atm. ($n = 2.445 \times 10^{19}$ cm^{-3})		Helium Vapor at 4.2 K P = 1 atm. ($n = 2.515 \times 10^{21}$ cm^{-3})		Helium Liquid at 4.2 K P = 1 atm. ($n = 1.878 \times 10^{22}$ cm^{-3})	
	α_r = 10^{-8} cm^{3}s^{-1}	α_r = 10^{-10} cm^{3}s^{-1}	α_r = 10^{-8} cm^{3}s^{-1}	α_r = 10^{-10} cm^{3}s^{-1}	α_r = 10^{-8} cm^{3}s^{-1}	α_r = 10^{-10} cm^{3}s^{-1}
Radiation-induced equilibrium ionization density N_0	3.578×10^7 cm^{-3}	3.578×10^8 cm^{-3}	3.628×10^8 cm^{-3}	3.628×10^9 cm^{-3}	2.147×10^9 cm^{-3}	2.147×10^{10} cm^{-3}
Time to reach 90% of equilibrium ionization density $t_{90\%}$	4.11 s	41.1 s	0.406 s	4.06 s	0.069 s	0.69 s

significant reduction in the value of the reduced breakdown potential $V_s'(N_o)$ over that of the full breakdown potential V_s. It is important to reiterate here that the WITAMIR central cell solenoids have more shielding than is necessary to satisfy the conventional radiation limits of the magnets. Therefore, in the case of a magnet which is fronted by an optimized shield and, therefore operating at one or more of the radiation limits, we would expect greater equilibrium ionization densities N_o than those given in Table 3.

Two dominant factors account for the high values of the equilibrium ionization density N_o in helium. First, the softening of the 14 MeV fusion neutron source by the intervening blanket and shield yields a neutron spectrum at the magnet which peaks around 1 MeV - see Fig. 5. This energy coincides almost exactly with the peak in the ^4He elastic scattering cross section σ. Therefore, the ionization production rate S, defined in Eq. (10), has a very large contribution from the product of $\sigma_g\phi_g$ for the energy group g centered around 1 MeV. Secondly, helium, being a noble gas, cannot form electronegative ions by electron attachment. The probability of electron-ion recombination is much lower than positive-negative ion recombination, with the result that helium exhibits very low values of the recombination coefficient α_r (10^{-8} to 10^{-10} cm^3 s^{-1}) compared with the polyatomic gases. Values of α_r in the range 10^{-6} to 10^{-7} cm^{-3} s^{-1} are typical for H_2 and O_2.

The fact that liquid helium exhibits higher equilibrium ionization densities N_o than those for the vapor phase is to be expected on two counts. Firstly, the number density n of the liquid phase is greater than the vapor phase and, from Eq. (14), N_o is proportional to $n^{1/2}$. Secondly, the mean energy W required to create an ion pair in the liquid phase of a noble gas is

only about two-thirds of the energy required in the vapor phase for the same incident particle energy.[12,35]

Note that if it becomes necessary to dump the stored energy of a superconducting magnet due to possible quenching, the fusion plasma would have to be rapidly shut down before attempting the magnet discharge. However, although the radiation source has been shut off, this does not necessarily mean that radiation-induced breakdown of the helium has been circumvented. That this is so can be by reference to the time constants for radiation-induced ionization density formation in Table 3. Due to the uniquely low values of the electron-ion recombination coefficients in helium, these time constants are seen to be as long as several tens of seconds, especially for helium in the vapor phase. Since the time constants for ionization decay after removal of the radiation field will be of the same order, radiation-induced ionization densities in helium can remain at appreciable levels even when the fusion plasma has been extinguished.

It is important here to notice that the radiation mechanism contributing to the radiation-induced breakdown of the helium medium in a superconducting magnet is <u>not</u> analogous to the mechanism which can induce damage in the epoxy or ceramic insulators of the same assembly. In the former the instantaneous neutron <u>flux</u>, or, equivalently, the ionization dose <u>rate</u>, must be sufficient to produce an appreciable steady state equilibrium ionization density N_o in the helium. In the latter, however, it is the neutron <u>fluence</u> (i.e., time integrated flux) which is important in that this can lead to chronic permanent radiation damage of the insulator structure. Radiation damage of helium, per se, is not possible. It can be seen, therefore, that radiation-induced electrical breakdown of helium becomes a potential problem as soon as the

fusion plasma reaches operating power. In this respect, this phenomenon is analogous to dose-rate resistivity degradation which can occur in ceramic insulators in high radiation fields.[57,58]

6.6 Additional Consequences

6.6.1 Pool-Boiling Versus Forced Flow. The fact that radiation fields may contribute to a significant reduction in the breakdown potential of helium has some important implications for the type of helium cryogenic system employed for fusion reactor superconducting magnet assemblies. In the pool-boiling system, saturated helium vapor is present in equilibrium with the liquid phase. Therefore, the reduction in the already low breakdown potential of the helium vapor in such systems, particularly at higher temperatures, may lead to their rejection in favor of the forced-flow supercritical cryogenic system with its all-liquid helium coolant.

6.6.2 Shielding Constraints for Mirror and Tokamak Magnets. Another consequence of these results is that radiation-induced breakdown of helium may prove to be the limiting factor in the shielding criteria for fusion reactor superconducting magnet systems (i.e., exceeding the shielding requirements for nuclear heating or chronic radiation damage). If so, this has some rather important implications for radiation-induced breakdown in the toroidal field (TF) coils of the current representative designs of future tokamak devices (e.g., UWMAK-III[1], STARFIRE,[2] INTOR,[45] FED,[51] etc.). Due to the nature of these tokamak designs, there is much less room for additional shielding between the first wall and the TF coils, than in the equivalent situation of additional shielding between the first wall and the central cell coils in the more conservative design of the tandem mirror reactor (see, for example, Ref.

42). The indication of deleterious radiation-induced breakdown in the tokamak TF coils may, therefore, warrant possible design modifications.

6.6.3 Radiation-Induced Breakdown in RF Transmission Systems. Finally, it is important to reiterate the associated implication of these results with regard to radiation-induced electrical breakdown in fusion RF heating systems discussed in Chapter 1. With the important exception of the quasi-optical launcher for electron-cyclotron resonance heating (ECRH) systems,[4] all other high power RF transmission systems rely on waveguides or coaxial feeds containing pressurized gases (typically N_2 or SF_6). Peak power densities within these systems typically span the range 10-100 kW cm^{-2} and employment of pressurized insulation gas significantly increases the electric field required for breakdown. In contrast to helium, N_2 and SF_6 do not exhibit such low values of the electron-ion recombination coefficient α_r and, additionally, may deliberately contain other electronegative impurities in order to maximize the voltage standoff capabilities. However, most RF transmission systems in conceptual fusion designs are routed to the wave launching point at or near the reactor first wall (see for example Refs. 1, 2 and 3) where radiation levels are several orders of magnitude greater than at the relatively well shielded superconducting magnets. Similar considerations of radiation-induced electrical breakdown will, therefore, be expected to apply. Studies of this phenomenon in fusion reactor RF systems are currently in progress.

7. CONCLUSIONS - THE NEED FOR FURTHER EXPERIMENTAL DATA

The experimental evidence discussed in Chapter 2 demonstrated that, under certain conditions, external radiation fields can influence the breakdown behavior of gases and liquids. The modified breakdown theory introduced in Chapter 5 showed that the reduction of the breakdown potential in the presence of a radiation field is strongly dependent on the ratio of N_0/N_c, where N_0 is the initial radiation-induced ionization density at equilibrium and N_c is the critical ionization density for the onset of streamer formation. Finally, the analysis performed in Chapter 6 demonstrated that the neutron-induced initial ionization density N_0 in the helium subsystem of a typical fusion reactor superconducting magnet is directly comparable to N_c and would be expected to contribute to a significant reduction of the breakdown potential in the helium medium.

Substitution of the expression for N_0 from Eq. (14) into Eq. (8) yields an expression for the reduced breakdown potential V_s' explicitly in terms of the incident multigroup neutron spectrum ϕ_g. However, the employment of the resulting expression to accurately predict the reduced breakdown potential in a specific helium system under irradiation conditions will not, at present, enable precise values to be obtained. This is due to the current paucity of adequate data for some of the constituent parameters for helium. These parameters include the first and second Townsend coefficients for liquid helium, and particularly the critical ionization density N_c and the recombination coefficient α_r for both liquid and gaseous helium.

In Section 6.5, it was reported that a wide range of α_r values for helium exist in the literature. This was reflected in the results in Table 3, where

the equilibrium ionization density N_0 was evaluated for a typical range of α_r from 10^{-8} to 10^{-10} cm^3 s^{-1}. Similarly, Section 5.5 showed that critical ionization densities in the range $N_c \sim 10^8$-10^{10} cm^{-3} would be expected at streamer initiation, but precise values would be expected to depend on the state of the medium and on the applied field. Such precise values do not exist in the literature.

The data base for liquid helium is particularly deficient. Measurements of the first and second Townsend coefficients (α and α/ω) have never been reported for this medium. The same is true for the recombination coefficient α_r. In fact, in view of the Dolgoshein effect in liquid noble gases where electrons created by ionizing events remain free to drift through the liquid with minimal recombination (see Section 4.4), the value of α_r in liquid helium may be much smaller than the range indicated above. In such a case, the equilibrium ionization density N_0 attained in the medium is likely to be considerably larger than that indicated in Table 3. Alternatively, this may be somewhat ameliorated by the fact that α_r may exhibit higher local values in the immediate vicinity of the slowing-down tracks of the neutron-induced recoil helium nuclei, where the ionization density of formation is initially very high.

It is therefore evident that a systematic set of experiments needs to be performed on liquid and gaseous helium in order that precise radiation-induced breakdown data may be evaluated for this dielectric. In view of the findings of this report, an urgent need exists for this experimental data for the successful design of fusion reactor superconducting magnet systems.

Acknowledgment

Support for this work has been provided by the U.S. Department of Energy.

REFERENCES

1. BADGER, B., et al., "UWMAK-III, A Noncircular Tokamak Power Reactor Design," University of Wisconsin Fusion Engineering Program Report UWFDM-150 (1976).

2. BAKER, C.C., et al., "STARFIRE - A Commercial Tokamak Fusion Power Plant Study," ANL/FPP-80-1, Argonne National Laboratory (1980).

3. LOGAN, B.G., et al., "Mirror Advanced Reactor Study (MARS) - Interim Design Report," UCRL-53333, Lawrence Livermore National Laboratory (1983). Final report to be published in 1984.

4. PERKINS, L.J., S.A. FREIJE, and W.S. NEEF, "Engineering Design of the Quasi-Optical ECRH Injection System for the Mirror Advanced Reactor," 5th Topical Meeting on the Technology of Fusion Energy, Knoxville, TN, April 1983. Also in Nuclear Technology/Fusion, September 1983.

5. ALLIBONE, T.E. and D. DRING, Proc. IEEE 120 No. 7 (1973) 815.

6. BOYLETT, F.D.A. and B.G. WILLIAMS, Brit. J. Appl. Phys. 18 (1967) 593.

7. FUCHS, W. and G. SCHUMACHER, Z. Phys. 112 (1939) 605.

8. BLAIR, D.T.A., F.M. BRUCE ad D.J. TELFORD, Proc. 6th Int. Conf. on Phenomena in Ionized Gases, Paris, Vol. 1, p. 321 (1963).

9. FALLOU, B., J. GARLAND and B. BOUVIER, Cryogenics 10 (1970) 142.

10. GUENTHER, A.H. and J.R. BETTIS, IEEE J. Quantum Elec. QE-3 No. 11 (1967) 581.

11. MORGAN F. and C. GREY-MORGAN, Proc. 9th Int. Conf. on Phenomena in Ionized Gases, Bucharest, p. 326 (1969).

12. PRICE, W.J., "Nuclear Radiation Detection," McGraw-Hill, 1964, p. 285

13. ALLKOFER, O.C., C. GRUPER and G. MAXION, Nucl. Inst. Meth. 79 (1970) 181.

14. GALAKTIONOV, Y.V., F.A. YECH, and V.A. LYUBIMOV, Nucl. Inst. and Meth. 33 (1965) 353.

15. CHANG, W.Y. and S. ROSENBLUM, Phys. Rev. 67 (1945) 222.

16. CONNOR, R.D., Proc. Phys. Soc. 864 (1951) 30.

17. GUPTA, S.L. and N.K. SAHA, Nucl. Inst. and Meth. 13 (1961) 258.

18. TOWNSEND, J.S., Nature 62 (1900) 340.

19. TOWNSEND, J.S., Phil. Mag. 1 (1901) 198.

20. PASCHEN, F., Weid. Ann. 37 (1889) 69.

21. GERHOLD, J., Cryogenics 12 (1972) 370.

22. MEATS, R.J., Proc. IEEE 119 No. 6 (1972) 760.

23. GONCHEROV, V.A., S.G. GOSTEEV, V.I. LEVITOV and V.Y. STAROBINSKII, Soviet Power Eng. 15 No. 1 (1977) 66.

24. LOEB, L.B., "Basic Processes in Gaseous Electronics," University of California Press, 1961, Chapter 9.

25. RAETHER, H., "Electrical Avalanches and Breakdown in Gases," Butterworths (London), 1964, Chapter 5.

26. DAVIDENKO, V.A., B.A. DOLGOSHEIN and S.V. SOMOV, Sov. Phys. JETP 28 (1969) 227.

27. LOZANSKII, E.D., Sov. Phys. - Tech. Phys. 13 (1969) 1269.

28. RICE-EVANS, P., "Spark, Streamer, Proportional and Drift Chambers," Richelieu Press (London), 1974.

29. BROWN, S.C., "Basic Data of Plasma Physics," Wiley (New York), 1959.

30. WILLIAMS, B.G., Proc. IEEE 121 No. 2 (1974) 161.

31. THARIS, J., A. DUBOIS and J.C. BOBO, Cryogenics 10 (1970) 147.

32. BLANK, C. and M.H. EDWARDS, Phys. Rev. 119 No. 1 (1960) 50.

33. OLIVER, G., IEEE Trans. Pwr. Appar. Syst. PAS-97 (1978) 969.

34. KRASUCKI, Z., Proc. Roy. Soc. A294 (1966) 393.

35. KNOLL, G.F., "Radiation Detectors and Measurement," Wiley, 1970, p. 748.

36. DERENZO, S.E., T.S. MAST and H. ZAKLAND, Phys. Rev. A9 (1974) 2582.

37. GROMOVA, I., V. NIKANOROV, G. PETER and V. PISAREV, Prib. Tekh. Eksp. 1 (1965) 64.

38. DOLGOSHEIN, B.A., JETP Lett. 11 (1970) 351.

39. HENNING, C.D., "Reliability of Large Superconducting Magnets Through Design," in Proc. of 1980 Conf. on Applied Superconductivity, Sante Fe, NM, USA, September 29 to October 2, 1980.

40. SCHMITT, F., G. METZGER, J. GRESSER, M. RIEDINGER and G. SUTTER, Nucl. Inst. and Meth. 76 (1969) 258.

41. WILKINSON, D.H., "Ionization Chambers and Counters," Cambridge University Press, 1950, p. 114.

42. WALTERS, R.T. and R.E. JONES, Proc. 5th Internat. Conf. on Phenomena in Ionized Gases, Munich, p. 992 (1961).

43. WALTERS, R.T. and R.E. JONES, Phil. Trans. Roy. Soc. 256A (1964) 185 and 213.

44. STEINER, D., Nucl. Sci. and Eng. 58 (1975) 107.

45. THE INTOR DESIGN TEAM, Nuclear Fusion 20 No. 3 (1980) 349.

46. SAWAN, M.E., "Charts for Specifying Limits on Copper Stabilizer Damage Rate," Proc. 3rd Top. Mtg. on Fusion Reactor Materials, Albuquerque, NM, Sept. 1983, to be published in J. Nucl. Mater.

47. GARBER, D.I. and R.R. Kinsey, "Neutron Cross Sections," BNL 325, Vol. II, p. 9, Brookhaven National Laboratory (1976).

48. PRICE, W.J., "Nuclear Radiation Detection," McGraw-Hill 1964, Chapter 1.

49. BADGER, B., et al. (29 authors), "WITAMIR-I, A University of Wisconsin Tandem Mirror Reactor Design," University of Wisconsin Fusion Engineering Program Report UWFDM-450 (Sept. 1980).

50. BORCHERS, R.R. and C.M. VAN ATTA (editors), "The National Mirror Fusion Program Plan," UCAR-10042-82, Lawrence Livermore National Laboratory (1982).

51. STEINER, D., W.R. BECRAFT and P.H. SAGER, J. Fusion Energy 1 No. 1 (1981) 5.

52. ENGLE, W.W., "ANISN, A 1-D Discrete Ordinates Code With Anisotropic Scattering," ORNL-K 1693, Oak Ridge National Laboratory (1973).

53. RSIC Data Library Collection DLC-41, Radiation Shielding Information Center, Oak Ridge National Laboratory.

54. HASTED, J.B., "Physics of Atomic Collisions," Butterworths (London) 1964.

55. WILKINSON, D.H., "Ionization Chambers and Counters," Cambridge University Press, 1950, p. 52.

56. MOTLEY, R.W. and A.F. KUCKES, Proc. 5th Internat. Conf. on Phenomena in Ionized Gases, Munich (1961).

57. PERKINS, L.J., "Radiation Dose-Rate Resistivity Degradation in Ceramic Insulators and Assessment of the Consequences in Fusion Reactor Applications," University of Wisconsin Fusion Engineering Program Report UWFDM-469 (1982).

58. PERKINS, L.J., "Materials Considerations for Highly Irradiated Normal-Conducting Magnets in Fusion Reactor Applications," Proc. 3rd Top. Mtg. on Fusion Reactor Materials, Albuquerque, NM, Sept. 1983. To be published in J. Nucl. Mater.